J. Astrophys. Astr. (1984) **5,** 43–53

The Radio Spectra of Galactic Centre Features

B. Y. Mills & M. J. Drinkwater *School of Physics, University of Sydney, N.S.W. 2006, Australia*

Abstract. The radio source Sgr A and neighbouring features have been mapped at a frequency of 843 MHz with a beamwidth of 43 × 87 arcsec. Comparisons have been made with published maps of comparable resolution at different frequencies in order to differentiate thermal and nonthermal regions. The arc feature to the north of Sgr A appears to consist of low-temperature ionized hydrogen and to extend partly over Sgr A itself causing patchy absorption at low frequencies; there is some evidence that the hydrogen in the arc has been expelled from the galactic nucleus. Previous suggestions that Sgr A East is a supernova remnant have been examined and the interpretation is found to be quite likely, but not compelling. The diffuse component of Sgr A West appears to be due entirely to ionized hydrogen surrounding the nucleus.

Key words: radio continuum—Sgr A—galactic centre

1. Introduction

Modelling of the emission sources associated with the galactic centre is fraught with difficulties. The distribution is complex at all scales of size and both thermal and nonthermal regions are almost inextricably mixed. Qualitatively a number of basic features can be recognized in the observed distribution. The integrated emission through the galactic disc forms a largely nonthermal ridge which stretches along the plane and has a half-brightness width of about 3 deg near the galactic centre. A disc-like nonthermal source, believed to be centred on the nuclear region, extends for two or three degrees along the plane on either side of the nucleus with a width of about half a degree; the emission appears to be strongly concentrated towards the nucleus. A similar but smaller distribution of ionized gas is also centred on the nucleus and extends for about $1\frac{1}{2}$ deg along the plane on either side; this is observed in absorption at very low frequencies and in emission at high frequencies. At high frequencies, also, several giant H II regions are observed in emission close to the nucleus. The dominant central source, Sgr A, embraces the accepted position of the nucleus and is the principal subject of the present investigation.

The brightness distribution of Sgr A is also complex and recognizable features depend strongly on the resolution and frequency of the observing telescope. At a resolution of ~ 1 arcmin we see the picture in Fig. 1, a bright centrally concentrated radio source with a faint arc-like feature extending to the north. At much higher resolutions, $\lesssim$ 5 arcsec, the arc disappears because of inadequate sensitivity but

structures in the central source become distinguishable (*e.g.* Ekers *et al.* 1983). A compact non-thermal source, coincident with the infrared (IR) source, is believed to represent the actual nucleus. Apparently associated with this is a bright spiral-like structure of ionized gas superimposed on a more extended diffuse feature with a flat but possibly non-thermal spectrum. This complex of features is called Sgr A West. A bright shell-like non-thermal source of diameter ~ 3 arcmin is centred about $1\frac{1}{2}$ arcmin to the east. It is designated Sgr A East and has been recognized as a possible supernova remnant. One side of this source coincides with the position of the Sgr A West maximum.

The present investigation makes use of observations with the Molonglo Observatory Synthesis Telescope (MOST) at a frequency of 843 MHz. We obtain some information about the unresolved components of Sgr A West but are principally concerned with spectral studies of well-resolved features, using for comparison purposes the 10.7 GHz map of Pauls *et al.* (1976) which has comparable solid angle resolution. Both maps are tied to a local zero of brightness but absolute values are needed for some purposes. Where necessary, these have been obtained making use of the lower resolution maps of Little (1974) at 408 MHz and Altenhoff *et al.* (1978) at 4.87 GHz. The 408 MHz data have also been very useful in helping to define the properties of the arc-like feature.

2. Map synthesis

The MOST has been described briefly by Mills (1981) and Durdin, Little & Large (1984). It is an east-west rotational synthesis array which uses a comb of fan beams to perform a synthesis in real time. The beams are formed using two co-linear parabolic reflectors each 780 m long by 11.6 m wide; they are directed in a north-south plane by rotating the reflectors about their long axis and in an east-west plane by phasing of the individual circularly polarized antenna elements at the line foci. To synthesize a map centred on a declination of – 29 deg, the maximum east-west beam swing is 61 deg which is the practical limit of the phasing system before marked deterioration sets in; there are already some problems of dynamic range evident in the synthesised map.

The region was observed on 1983 February 24 using a field size of 46 × 46 cosec δ arcmin. The synthesised beamwidth was 43 × 87 arcsec to half power with a negative sidelobe of –8 per cent. The effects of this and other sidelobes (< 1 per cent) were removed from the map using a standard cleaning process (Crawford 1984). The map was cleaned to 1.5 per cent of the peak and restored using the positive lobe of the actual beam. The resulting map is shown in Fig. 1.

The map zero is not well defined: it is depressed by an amount proportional to the 'uncleaned' emission received by the 2 deg fan beams and—near the galactic centre—this emission is substantial. The comparison map at 10.7 GHz has similar but less severe problems (Pauls *et al.* 1976). It has been tied to a local zero and there is also a weak positive 'spill-over' from the strong Sgr A response. For comparison we have chosen an effective zero for the MOST map at – 1.5 per cent of the Sgr A positive peak or at –0.37 Jy/beam. The zero was chosen to match as nearly as possible the zero of the 10.7 GHz map. The contour unit on the map is 1 per cent of the positive peak deflection and corresponds to a brightness temperature of T_B = 133 K.

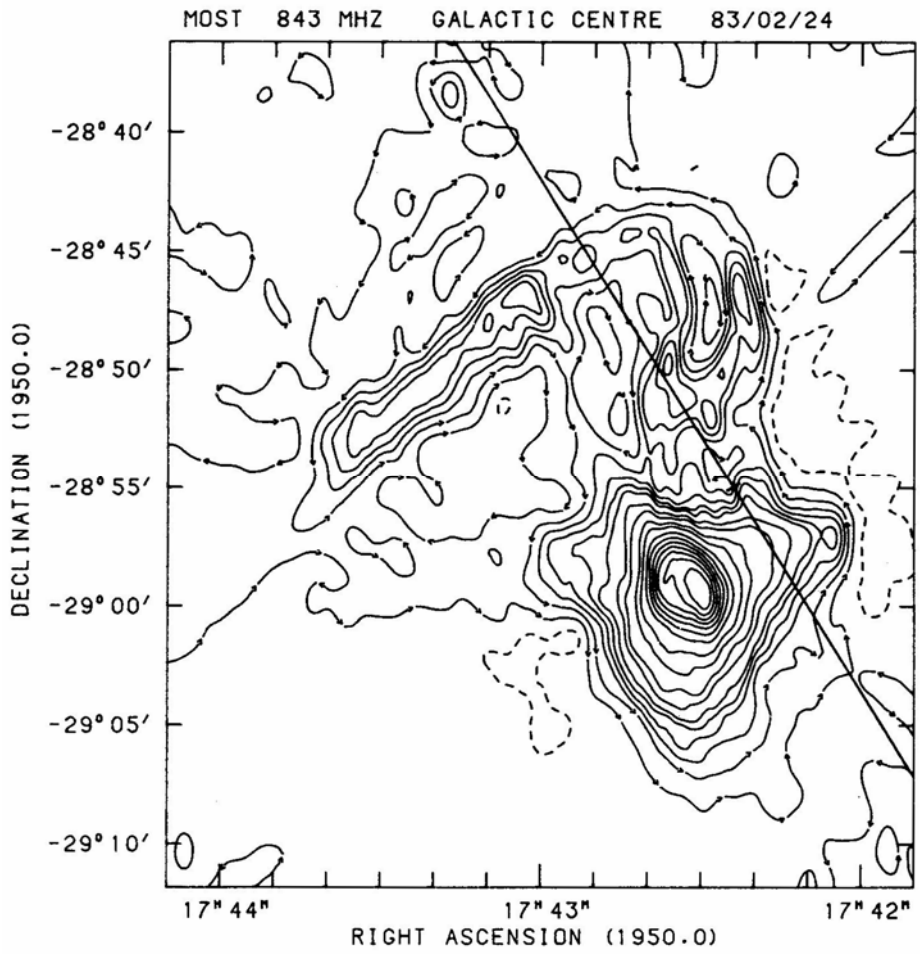

Figure 1. Cleaned MOST map of the emission near Sgr A at 843 MHz. The contours are at – 1 (dashed), 0, 1, 2, 3, 4, 5, 7.5, 10, 15, 20, 30 . . . 90 percent of the peak brightness of 24.9 Jy/beam (13300 K). The half-power ellipse of the MOST beam is given in the bottom left corner. The galactic equator ($b = 0$) is also shown.

3. The arc region

The most striking feature in Fig. 1 is the arc-like structure which extends northwards from the main peak of Sgr A and then bends sharply to cross the galactic plane in a south-easterly direction. The northerly extension breaks into two clearly defined ridges of emission which are also evident in the 10.7 GHz map of Pauls *et al.* (1976). A third very weak ridge, not evident at 10.7 GHz, is probably unassociated with the arc, possibly even an artefact.

Because the brightness of the arc feature is very low compared with Sgr A itself, there are some problems associated with determining its spectrum. Three well-defined maxima in the arc emission have been chosen, G 0.16 – 0.15, G 0.18 – 0.04 and G 0.10 + 0.18. From cross-sections of the arc constructed from the contour diagrams at these

Table 1. Spectra of three well-defined maxima in the arc emission.

	ΔT(K)			α	
	408 MHz	843 MHz	10.7 GHz	10.7–0.843	10.7–0.408
G 0.16−0.15	2900	690	4.3	−0.01	+0.01
G 0.18−0.04	2400	760	5.0	+0.02	+0.11
G 0.10+0.08	2000	640	3.5	−0.05	+0.06

positions, local zeros and the temperature excess due to the arc have been estimated. The excess temperatures, ΔT, are given in Table 1, together with the effective spectral index, α between 10.7 GHz and 843 MHz, defined by $\Delta T \propto \nu^{\alpha-2}$. Further information about low-frequency spectra has been obtained from the 408 MHz map of Little (1974). Applying a similar procedure the corresponding results are also listed in Table 1.

It is evident that the spectra are consistent with thermal emission from ionized hydrogen. The optical depths of all regions appear to be small but significant, particularly at 408 MHz.

In principle the electron temperature and emission measure of the H II regions may be obtained from these results although high accuracy cannot be expected. For a uniform H II region of electron temperature T_e and optical depth τ observed in front of a region of uniform brightness temperature T_B we have

$$\Delta T = (T_e - T_B)\,(1 - e^{-\tau}).$$

We adopt T_B = 1700 K at 408 MHz based on the map of Little (1974) on the assumption that slightly more than half the extended emission in the direction of the arc originates behind it. Although appreciably lower at 843 MHz, T_B turns out to be significant at this frequency also. We adopt a spectral index, α = – 0.3, based on comparison with the appropriate map of Altenhoff *et al.* (1978) at 4.87 GHz; at 843 MHz this gives T_B = 320 K. Using these estimates of T_B and the relation $\tau \propto \nu^{-2.09}$ (based on the variation of Gaunt factor over this frequency range) we have solved for T_e and τ at 408 MHz and 843 MHz in conjunction with the 10.7 GHz measurements. These results are shown in Table 2, together with the emission measures calculated from the estimated 10.7 GHz temperatures on assuming an electron temperature of 6000 K.

There is considerable scatter in the derived electron temperatures but this is understandable in view of the uncertain estimates of ΔT and T_B; the results are consistent with a mean temperature of about 6000 K. The temperatures of 6000–12000 K deduced from radio recombination-line measurements (Pauls *et al.* 1976; Pauls & Mezger 1980) are higher and no line could be detected at the position of

Table 2. Derived properties for three maxima in the arc emission.

	T_e(K)		τ		EM
	408 MHz	843 MHz	408 MHz	843 MHz	× 10^4
G 0.16−0.15	12000	3800	0.32	0.22	13
G 0.18−0.04	6500	3000	0.70	0.33	15
G 0.10+0.08	7300	7500	0.45	0.09	11

G 0.16–0.15, leading to the suggestion that the emission here is nonthermal. An underestimate of the underlying nonthermal emission may contribute to an overestimate of temperatures using radio recombination lines and—in view of all the uncertainties—we do not believe that the discrepancies are significant. To account for the failure to detect line radiation in G 0.16–0.15, a high electron temperature and/or a large velocity dispersion may be needed in addition. There can be little doubt that the latter source is largely thermal. A possible reason for an underestimate of the nonthermal component of brightness is a ridge of emission which can be recognized extending for about two degrees across and approximately normal to the plane close to the longitude of the arc feature. Comparison of the data of Little (1974) and Altenhoff *et al.* (1978) indicates that the ridge has a non-thermal spectrum with $\alpha \sim -0.6$, compatible with the general galactic radiation. This ridge is an unusual feature and as it is almost coincident with another unusual feature, the arc, the possibility of a physical association might be considered. However, we can suggest no plausible physical connection.

The mass of gas in the whole arc feature may be estimated roughly by adopting a mean emission measure of 6×10^4 and a model comprising a long cylinder lying in a plane perpendicular to the line of sight. An inclination of the plane increases the derived mass and an allowance for a filling factor decreases it. The model yields a mass M ~5000 $M_\odot$.

What then is the nature of the arc? The entire feature appears to be a region of ionized hydrogen with little or no associated nonthermal emission. Interpretation as a simple spiral feature inclined to the galactic plane seems impossible, even allowing for gas motion along the spiral, because of the distribution of radial velocities determined from radio recombination lines (Pauls *et al.* 1976; Pauls & Mezger 1980). These show a velocity $\lesssim -40$ km s^{-1} just north of Sgr A increasing to zero at the bend in the arc and rising further to + 40 km s^{-1} at the position of G 0.18 – 0.04. Such a pattern could be generated by an expanding ring or, perhaps more plausibly, by a precessing jet of ionized hydrogen arising in the nuclear region. The latter would involve much lower expulsion velocities than usually associated with jets (~ 100 km s^{-1}) but the shape of the feature, particularly the sharp bend followed by the straight south-westerly extension, can be readily modelled. The estimated age of such a feature at its extremity would be ~ 10^6 yr, roughly the same as the precession period, and the rate of expulsion of matter, $M \sim 5 \times 10^{-3}\ M_\odot$ yr^{-1}.

A precessing jet model on a much smaller scale has been proposed by Brown (1982) to account for the spiral-like structure of the thermal component of Sgr A West, but his derived parameters are incompatible with the arc feature; the precession period is shorter by two or three orders of magnitude and the precession is in the opposite sense. It seems that there is no simple model tying together these features but nevertheless an association of the arc feature with the nucleus appears likely.

4. Sagittarius A

For the purposes of analysis we define Sgr A as the emission region south of declination – 28° 54′. The sources conventionally named Sgr A East and Sgr A West are not separately resolved in Fig. 1 although the beginnings of the ring structure of Sgr A East can be recognised; these bright central sources are surrounded by an extensive low-

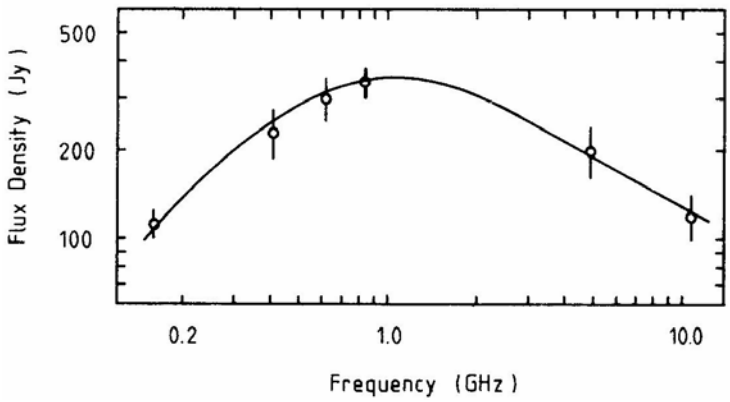

Figure 2. Radio spectrum of Sgr A, based on observations with resolution better than 3 arcmin. (Data sources are, 160 MHz: Dulk & Slee 1974; 408 MHz: Little 1974; 610 MHz: Downes *et al.* 1978; 843 MHz: this work; 4.875 GHz: Downes *et al.* 1978; 10.7 GHz: Pauls *et al.* 1976.)

brightness region. The 843 MHz appearance is qualitatively similar to the 10.7 GHz map of Pauls *et al.* (1976), although a detailed comparison reveals great variations in spectral index. At 843 MHz, the integrated flux density is 340 Jy. The spectrum of Sgr A between 10 GHz and 160 MHz is given in Fig. 2; the high frequency spectral index is $\alpha \simeq -0.57$. The low frequency turnover suggests absorption from intervening ionized hydrogen with a patchy distribution and a mean emission measure of $\sim 7 \times 10^4$, similar to the mean emission measure of the arc feature.

4.1 *Spectral Index Distribution*

The distribution of spectral index across Sgr A has been derived from a comparison of the present map with the 10.7 GHz map of Pauls *et al.* (1976). A zero level of – 1.5 per cent has been adopted for the 843 MHz map, as discussed in Section 2, and comparisons have been made only when the derived brightness is more than 4 per cent of the peak. This largely avoids problems associated with uncertainty of the mean zero level and its possible variation over the map. The derived contours of α are shown in Fig. 3.

Although the accuracy is poor, there is clearly a north-south gradient in α, evidently indicating a gradient in the proportion of thermal emission. On the northern border the emission is dominated by the ionized hydrogen which continues northwards to form the arc. The central region of low α is associated with the bright Sgr A East source which contributes most of the emission. Also there appears to be a real lack of hydrogen just north of this source, whereas the adjacent Sgr A West shows clearly a pocket of high α, undoubtedly associated with a concentration of ionized hydrogen around the nucleus. It appears that the nonthermal index of the fainter extended emission is $\alpha \simeq -0.7$ but, because of the zero level problem, the uncertainty is large. This emission appears to be associated with the nucleus and may represent the central peak of the extended non thermal source which stretches for some 5 deg along the galactic plane.

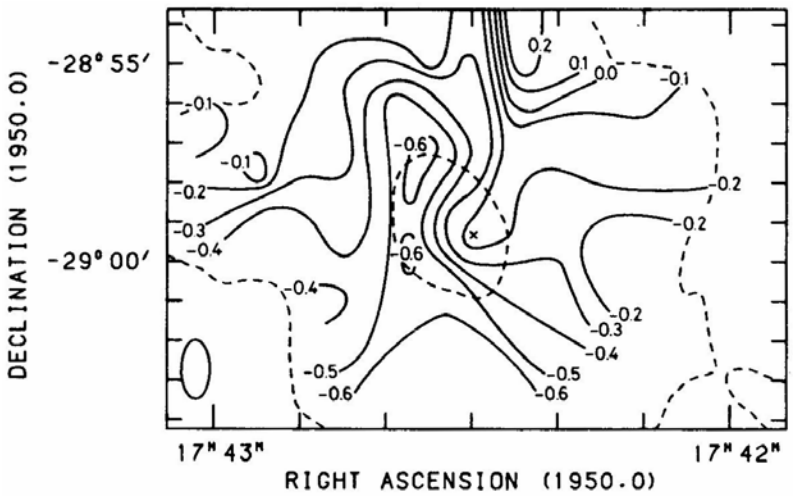

Figure 3. Distribution of spectral index near Sgr A, measured between 843 MHz and 10.7 GHz. The zero and 50 per cent contours of Fig. 1 are shown dashed and the position of Sgr A West is indicated.

4.2 *Sgr A East*

The central Sgr A concentration is an elliptical source with the major axis parallel to the galactic plane. The two components are not clearly resolved in the map of Fig. 1 but comparisons of cross-sections through the source at 843 MHz and 10.7 GHz shown in Fig. 4 indicate the two regions of different spectra. These agree closely with the detailed VLA maps presented by Ekers *et al.* (1983). The 10.7 GHz–843 MHz spectral indices at the centres of the East and West sources are α (East) = – 0.56 and α (West) = – 0.17.

The eastern source has been known for some time to have a ring-like structure and the possibility that it is a supernova remnant (SNR) has been discussed by several authors (Jones 1974; Gopal-Krishna & Swarup 1976; Goss *et al*., 1983). The strongest case has been made out by Goss *et al*, who used VLA observations which demonstrate a morphology similar to that of many SNRs; the spectral index is also compatible. If the source is a SNR situated on a line of sight that passes close to the nucleus, the question of its distance arises. Is it a chance alignment or is it actually in the central region? Goss *et al.* (1983) conclude that it is most probably within the nuclear bulge, at least. Using the results of Mills *et al.* (1984) we find that a typical remnant having the properties of Sgr A East would have an even chance of being located within about 2–3 kpc of the nucleus, on either side. As the occurrence of a supernova is a chance event proportional to the local stellar density, a location in the central region is very much more probable than any other single location along the line of sight, but the probability is still low.

X-ray observations by Watson *et al.* (1981) provide further clues. Several X-ray sources, including Sgr A West, were detected close to the nucleus but no source was found at the position of Sgr A East. If this were a typical small-diameter SNR (< 10 pc), the data of Long, Helfand & Grabelsky (1981) on the LMC supernova remnants would suggest a high luminosity, $\sim 10^{37}$ erg s^{-1} in the energy range 0.15–4.5 keV. However, the absorption is also high; Watson *et al.* estimate that the hydrogen column density to the nucleus lies between 2×10^{22} and 10^{23} cm^{-2}. Detection of a SNR near the nucleus

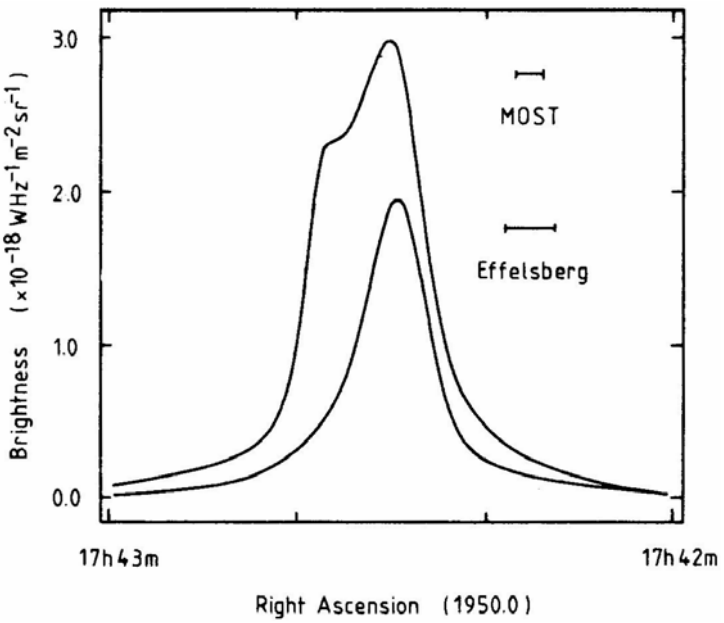

Figure 4. Gross-sections in R.A. of Sgr A at 843 MHz (upper curve) and 10.7 GHz (lower curve). The respective half-power beamwidths are shown.

with the above luminosity might be expected at the lower extreme of density, but not at the higher. Thus no positive conclusion is possible although a location much in front of the nucleus would seem to be unlikely. For a typical SNR the results of Mills *et al.* (1984) imply an age of ~ 300 yr and a possible expansion rate of ~ 0.1 arcsec yr^{-1}; proper motion studies may be profitable before long. However, if the supernova were located in the dense environment close to the galactic centre it is most unlikely that these results would be applicable and an old slowly expanding remnant might be expected.

Finally, we must consider the possibility that the source is not a supernova remnant. The positional coincidence of the nucleus and the brightest side of the source, together with the symmetry about the minor axis, does suggest a possible physical relationship to the nucleus, but the form this relationship might take is unclear. Further speculation is pointless at present; eventually polarization data may contribute to an understanding of the source.

4.3 *Sgr A West*

Ekers *et al.* (1983) describe three features associated with Sgr A West, a compact non-thermal source coincident with an infrared source and believed to represent the nucleus, a spiral feature of bright ionized hydrogen and a diffuse source of 'non-thermal' emission of spectral index $\alpha \simeq -0.3$ centred on the nucleus. The compact source is weak and irrelevant to the present observations. The diffuse 'non-thermal' source is located in Fig. 3 in the region of flattish spectral index coincident with the nucleus (peak $\alpha = -0.17$). We prefer to interpret it as a thermal source superimposed on the non-thermal Sgr A East; that is, we attribute the excess emission to diffuse ionized hydrogen

surrounding the nucleus. There appears to be no need to introduce another class of non-thermal sources with a different spectral index, either here or to interpret the VLA results. With this interpretation it is possible to model the emission and obtain information about the possible locations of Sgr A East with respect to the nucleus.

Three models have been examined in which (1) Sgr A East is located in front of the nucleus, (2) Sgr A East is behind the nucleus, and (3) the western part of Sgr A East is located at the nucleus and surrounds the thermal source. We assume that the thermal source has dimensions given by the region of flattest spectral index in the distribution of Ekers *et al.* (1983), that is a projected area of 0.33 arcmin^2, which is approximately 2/5 of the Molonglo beam size. The depth is taken as equal to the average width of the distribution $\simeq 0.7$ pc.

(1) The brightness temperature at 843 MHz is given by

$$T'_{.843} = \beta_M T_e (1 - e^{-\tau}) + T_{.843},$$

where $\beta_M = 0.4$ is the fraction of the Molonglo 843 MHz beam occupied by the thermal source, T_e is the electron temperature of the thermal source and $T_{.843}$ is the brightness temperature of the adjacent region of Sgr A East. A similar equation may be applied to the 10.7 GHz map of Pauls *et al.* (1976), when we have

$$T'_{10.7} = \beta_E T_e \tau + T_{10.7},$$

where $\beta_E = 0.26$ is the fraction of the Effelsberg 10.7 GHz beam occupied by the thermal source. Assuming $\tau \propto \nu^{-2.1}$ and $T_\nu \propto \nu^{-2.56}$, these equations may be solved to give $T_e = (7600 \pm 2000)$ K and $\tau_{.843} = 4 \pm 2$. The derived mass for a uniform model is $M = (70 \pm 30)\, M_\odot$.

(2) The expression for the 843 MHz brightness temperature now becomes

$$T'_{.843} = \beta_M [T_e(1 - e^{-\tau}) + T_{.843}\, e^{-\tau}] + (1 - \beta_M) T_{.843}.$$

Solving as before, we find $T_e \sim 20000$ K and $\tau_{.843} \sim 1.5$ with considerable uncertainty. The derived mass is $M \sim 100\, M_\odot$.

(3) With the thermal source surrounded by the nonthermal Sgr A East we have

$$T'_{.843} = \beta_M [T_e (1 - e^{-\tau}) + T_{.843} (1 + e^{-\tau}) (l - s)/2l] + (1 - \beta_M) T_{.843},$$

where s is the depth of the thermal source and l is the depth of the non-thermal source. From the maps of Ekers *et al.* (1983) we estimate $s/l \simeq 1/7$. Solving, we then find $T_e = (13000 \pm 3000)$ K and $\tau_{.843} = 2.4 \pm 0.7$. The mass of the ionized hydrogen is $M = (80 \pm 30)\, M_\odot$.

The derived electron temperature is very sensitive to the location of Sgr A East. In view of the uncertainties, none of the models can be rejected, but a location behind the nucleus is less plausible because of the necessary high electron temperature. On the other hand the derived mass of the H II region is insensitive to location and appears to be $\sim 80\, M_\odot$, in reasonable agreement with the high frequency VLA results of Brown & Johnston (1983).

Although the spiral feature is too small for a recognizable contribution to the present results, the data of Ekers *et al.* (1983) suggest to us a model which apparently has not been considered. Qualitatively, the shape of the feature and the pattern of velocities measured in the Ne II line at 12.8 μm (Lacy *et al.*, 1980) could be explained by a model comprising a precessing northwards flowing jet, combined with a rapidly rotating accretion disc into which gas flows from the galactic plane along distorted paths, of

which we observe the regions of greatest optical depth. The rate and direction of the precession required to account for the velocity distribution along the jet is, however, not compatible with the jet model of the arc discussed in Section 3. Further velocity data would be needed to explore the model quantitatively.

5. Conclusions

Observations of the galactic centre with a resolution of ~ 1 arcmin over a wide frequency range provides information supplementary to the high-resolution VLA observations and, in particular, it removes some uncertainties of interpretation resulting from the absence of low spatial frequencies. Our conclusions may be summarized as follows:

(1) The northern arc feature is an elongated distribution of ionized hydrogen, probably of rather low temperature. Modelling of the velocity field is difficult but it does fit a picture of a low-velocity 'precessing' jet arising in the nuclear region; it does not fit a simple spiral structure.

(2) The integrated spectrum of Sgr A shows evidence for patchy absorption of ionized hydrogen. The greatest concentration of hydrogen is located at the position of the galactic nucleus, but otherwise, it increases northwards in the direction of the arc.

(3) Sgr A East remains a problem. Interpretation as a supernova remnant within, or possibly in front of, the nuclear region seems most likely but a possible interpretation as a source deriving from the nucleus cannot be excluded.

(4) Sgr A West is most simply interpreted as a thermal source plus the very compact non-thermal component identified with the nucleus itself. We are inclined to believe that the spiral feature evident in VLA maps may combine both accretion and ejection but cannot directly associate it with the northern arc structure, with which it does have some features in common.

Acknowledgements

Operation of the Molonglo Observatory Synthesis Telescope is supported by the Australian Research Grants Scheme and by the University of Sydney.

References

Altenhoff, W. J., Downes, D., Pauls, T., Schraml, J. 1978, *Astr. Astrophys. Suppl. Ser.*, **35,** 23.

Brown, J. L. 1982, *Astrophys. J.*, **262,** 110.

Brown, R. L., Johnston, K. J. 1983, *Astrophys. J.*, **268,** L85.

Crawford, D. F. 1984, *URSI/IAU Symp. on Measurement and Processing for Indirect Imaging* (in press).

Downes, D., Goss, W. M., Schwarz, U. J., Wouterlout, J. G. A. 1978, *Astr. Astrophys. Suppl. Ser.*, **35,** 1.

Dulk, G. A., Slee, O. B. 1974, *Nature*, **248,** 33.

Durdin, J. M., Little, A. G., Large, M. I. 1984, *URSI/IAU Symp. on Measurement and Processing for Indirect Imaging* (in press).

Ekers, R. D., van Gorkom, J. H., Schwarz, U. J., Goss, W. M. 1983, *Astr. Astrophys.*, **122,** 143.

Gopal-Krishna, Swarup, G. 1976, *Astrophys. Lett.*, **17,** 45.
Goss, W. M., Schwarz, U. J., Ekers, R. D., van Gorkom, J. H. 1983, in *IAU Symp.* 101: *Supernova Remnants and their X-ray Emission*, Eds J. Danziger and P. Gorenstein, D. Reidel, Dordrecht, p. 65.
Jones, T. W. 1974, *Astr. Astrophys*., **30,** 37.
Lacy, J. H., Townes, C. H., Geballe, T. R., Hollenbach, D. J. 1980, *Astrophys. J*., **241,** 132.
Little, A. G. 1974, in *IAU Symp.* 60: *Galactic Radio Astronomy,* Eds F. J. Kerr and S. C. Simonson III, p. 491.
Long, K. S., Helfand, D. J., Grabelsky, D. A. 1981, *Astrophys. J*., **248,** 925.
Mills, B. Y. 1981, *Proc. astr. Soc. Aust*., **4,** 156.
Mills, B. Y., Turtle, A. J., Little, A. G., Durdin, J. M. 1984, *Aust. J. Phys.* (submitted).
Pauls, T., Downes, D., Mezger, P., G., Churchwell, E. 1976, *Astr. Astrophys.*, **47,** 407.
Pauls, T., Mezger, P. G. 1980, *Astr. Astrophys.*, **85,** 26.
Watson, M. G., Willingale, R., Grindlay, J. E., Hertz, P. 1981, *Astrophys. J.*, **250,** 142.